





Bond-weighted tensor renormalization groupDaiki Adachi ¹, Tsuyoshi Okubo ^{2,3} and Syngae Todo ^{1,2,4}¹*Department of Physics, University of Tokyo, Tokyo 113-0033, Japan*²*Institute for Physics of Intelligence, University of Tokyo, Tokyo 113-0033, Japan*³*JST, PRESTO, Kawaguchi 332-0012, Japan*⁴*Institute for Solid State Physics, University of Tokyo, Kashiwa, 277-8581, Japan* (Received 18 November 2020; revised 27 December 2021; accepted 5 January 2022; published 3 February 2022)

We propose an improved tensor renormalization-group (TRG) algorithm, the bond-weighted TRG (BTRG). In BTRG, we generalize the conventional TRG by introducing bond weights on the edges of the tensor network. We show that BTRG outperforms the conventional TRG and the higher-order tensor renormalization group with the same bond dimension, whereas its computation time is almost the same as that of TRG. Furthermore, BTRG can have nontrivial fixed-point tensors at an optimal hyperparameter. We demonstrate that the singular value spectrum obtained by BTRG is invariant under the renormalization procedure in the case of the two-dimensional Ising model at the critical point. This property indicates that BTRG performs the tensor contraction with high accuracy whereas keeping the scale-invariant structure of tensors.

DOI: [10.1103/PhysRevB.105.L060402](https://doi.org/10.1103/PhysRevB.105.L060402)

Since Onsager proved the existence of a phase transition in the two-dimensional Ising model in 1944 [1], critical phenomena have been one of the central subjects in statistical physics and condensed-matter physics. However, since only a few models have exact solutions, we generally need to conduct numerical simulations or approximated analytical calculations to investigate phase transitions and critical properties observed in exotic statistical models and materials. Among various numerical techniques, the numerical renormalization-group method based on the tensor network representation has become popular recently after the tensor renormalization group (TRG) proposed by Levin and Nave in 2007 [2]. In TRG, we represent the partition function as a tensor network and perform tensor contractions using the low-rank approximation based on the singular value decomposition (SVD). This technique enables us to evaluate the partition function and related physical quantities quite accurately for exponentially large systems, which can be regarded virtually as in the thermodynamic limit. TRG and its variants have been successfully used to investigate a wide range of classical and quantum many-body systems [3–12].

It has been widely realized, however, that TRG becomes less accurate near the critical points. To improve the accuracy of the numerical renormalization group for critical systems, the researchers have developed several algorithms so far. For example, the second renormalization group (SRG) [13] considers the low-rank approximation of the local tensors by taking the effect of environment tensors into account. It has been demonstrated that SRG successfully improves accuracy, although it is much more expensive computationally [14].

Another example is the higher-order tensor renormalization group (HOTRG) [15], which uses the higher-order singular value decomposition (HOSVD) instead of SVD. The accuracy of HOTRG is higher than the conventional TRG but lower than SRG. One can understand the reason for the

increased accuracy of HOTRG than TRG because HOTRG applies the HOSVD low-rank approximation to a pair of tensors. It might also be natural that the accuracy of SRG is higher than HOTRG because SRG performs the low-rank approximation under a larger approximate environment.

More recently, the accuracy of the tensor network algorithms is discussed from the viewpoint of short-range loop entanglement. In TRG, the loop entanglement, which represents short-range correlations in the physical systems, remains and accumulates during the renormalization steps. By eliminating the effects of the loop entanglement directly, several methods achieved higher accuracy even near the critical point [16–26].

Although the proposed methods produce more accurate results than the original TRG, they require significantly higher computation cost at the expense. If one can improve the accuracy without increasing the computation cost, it will expand the applicability of the tensor network algorithms to problems that were previously difficult to apply. An example of such methods might be the anisotropic tensor renormalization group (ATRG), which is recently proposed as the real-space renormalization group for hypercubic lattices in general dimensions [27]. In Ref. [27], the present authors showed that without increasing the leading computation costs, ATRG improves the accuracy for the case of the two-dimensional Ising model.

In this Letter, we propose another improved TRG algorithm, the bond-weighted tensor renormalization group (BTRG), which achieves much higher accuracy than the conventional TRG without increasing the computation cost. In BTRG, we introduce bond weights on the edges of the tensor network. We demonstrate that in the case of the two-dimensional Ising model, BTRG outperforms the conventional TRG and HOTRG. Interestingly, the singular value spectrum at the critical point, obtained by BTRG with an

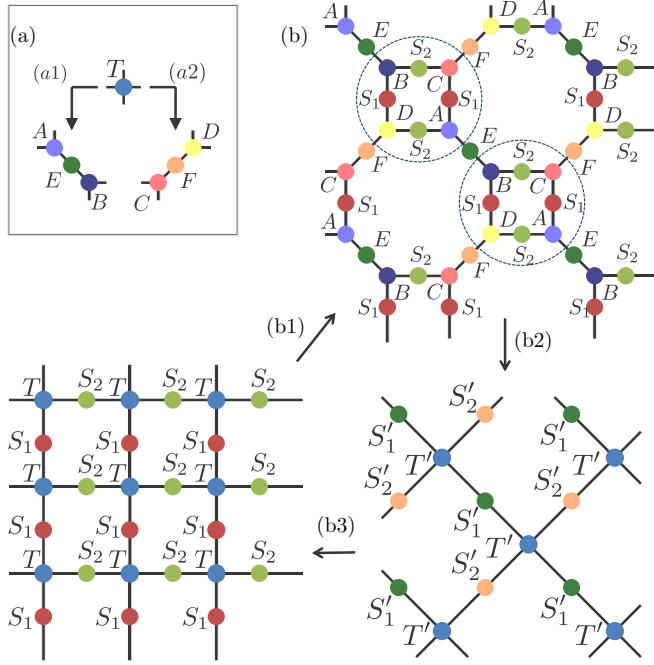


FIG. 1. (a) Tensor decompositions in BTRG. A rank-4 site tensor (T) is decomposed into two rank-3 tensors (A and B or C and D) and one rank-2 tensor (E or F) depending on the position in the tensor network. Decompositions (a1) and (a2) correspond to Eqs. (1) and (2), respectively. (b) Renormalization step of BTRG. (b1) Tensor decomposition: Each rank-4 tensor is decomposed into two rank-3 tensors and one rank-2 tensor, according to (a1) or (a2). (b2) Tensor contraction: Four rank-3 tensors (A – D) and four rank-2 tensors (two S_1 's and two S_2 's) are contracted into a new site tensor (T'), and the remaining tensors (E and F) are regarded as new bond tensors (S'_1 and S'_2) [Eqs. (9)–(11)]. (b3) Rescale: by rotating the new network by $\pi/4$ and rescaling by a factor of $1/\sqrt{2}$, the original square-lattice structure is retained. In these network diagrams, the bond dimension of the legs (solid lines) is all χ 's,

optimal hyperparameter, is stable under the renormalization procedure. This observation indicates that BTRG captures the correct scale-invariant property of renormalized tensors at the critical point [16].

In BTRG, we consider renormalization of a tensor network with tensors locating not only on the vertices (sites), but also on the edges (bonds) (see Fig 1). BTRG's renormalization process is slightly different from conventional TRG. In the original TRG, a rank-4 site tensor is decomposed into two rank-3 tensors. On the other hand, in BTRG, a rank-4 site tensor is decomposed into two rank-3 tensors and one rank-2 tensor as shown in Fig. 1(a).

Similar to the conventional TRG, first we apply the low-rank approximation to the 4-rank site tensor by using SVD. We introduce the following two different decompositions depending on the position in the tensor network [Fig. 1(a)]:

$$T_{x_0, x_1, y_0, y_1} \approx \sum_i^\chi U_{1(x_0, y_0), i} \sigma_{1ii} V_{1i, (x_1, y_1)}, \quad (1)$$

$$T_{x_0, x_1, y_0, y_1} \approx \sum_i^\chi U_{2(x_0, y_1), i} \sigma_{2ii} V_{2i, (x_1, y_0)}, \quad (2)$$

where χ is the cutoff of the bond dimension. Then, we define the tensors A – F as

$$A_{(x_0, y_0), i} = U_{1(x_0, y_0), i} \sigma_{1ii}^{(1-k)/2}, \quad (3)$$

$$E_{i, j} = \delta_{ij} \sigma_{1ii}^k, \quad (4)$$

$$B_{i, (x_1, y_1)} = \sigma_{1ii}^{(1-k)/2} V_{1i, (x_1, y_1)}, \quad (5)$$

$$C_{(x_0, y_1), i} = U_{2(x_0, y_1), i} \sigma_{2ii}^{(1-k)/2}, \quad (6)$$

$$F_{i, j} = \delta_{ij} \sigma_{2ii}^k, \quad (7)$$

$$D_{i, (x_1, y_0)} = \sigma_{2ii}^{(1-k)/2} V_{2i, (x_1, y_0)}. \quad (8)$$

Here, k is a hyperparameter representing the difference from the original TRG. The present algorithm is reduced to the original TRG at $k = 0$. In the case of TRG ($k = 0$), E and F [Eqs. (4) and (7)] are identity matrices, whereas for nonzero k , they contain information about the singular values. After the decompositions of the rank-4 tensors, we create new renormalized site tensors by contracting four rank-3 tensors and four rank-2 tensors, and regard E and F as new bond tensors as

$$T'_{x_0, x_1, y_0, y_1} = \sum_{i_0, i_1, i_2, i_3} [B_{x_0, (i_0, i_2)} C_{(i_0, i_3), y_0} D_{y_1, (i_1, i_2)} \times A_{(i_1, i_3), x_1} S_{2i_0, i_0} S_{2i_1, i_1} S_{1i_2, i_2} S_{1i_3, i_3}], \quad (9)$$

$$S'_1 = E, \quad (10)$$

$$S'_2 = F. \quad (11)$$

By rotating the new network by $\pi/4$ and rescaling by a factor of $1/\sqrt{2}$, the original square-lattice structure is retained. We present the whole renormalization step of BTRG in Fig. 1(b). It is straightforward to confirm that the order of the costs of this algorithm is the same as the original TRG: It requires $O(\chi^5)$ computation cost and $O(\chi^3)$ memory footprints.

As an initial condition, we set the bond tensors S_1 and S_2 as identity matrices at the beginning of BTRG. During the renormalization steps, they become nontrivial through the singular values of σ^k of the site tensors. The extra weights of the singular values $\sigma^{-k/2}$ are included in A – D tensors in addition to the weight $\sigma^{1/2}$ in the original TRG. We may consider these weights as a mean-field environment similar to the mean-field SRG proposed in Ref. [14]. In the mean-field SRG, one estimates the mean field by iterative calculations, whereas in BTRG, we use the singular values obtained in the previous step. Thus, no additional effort is required for estimating the environment. Nevertheless, BTRG with a proper choice of k dramatically improves the accuracy as shown below.

To demonstrate the advantage of BTRG, we calculate the two-dimensional Ising model on the square lattice by three different methods, TRG, HOTRG, and BTRG, and compare their results. The initial site tensor is prepared in the same way as described in Ref. [15]. The renormalization is performed 16 times for each axis for HOTRG and 32 times for TRG and BTRG. Thus, we calculate the partition function of the Ising model on $2^{16} \times 2^{16}$ square lattice with the periodic boundary condition. First, we examine the k dependence of the relative

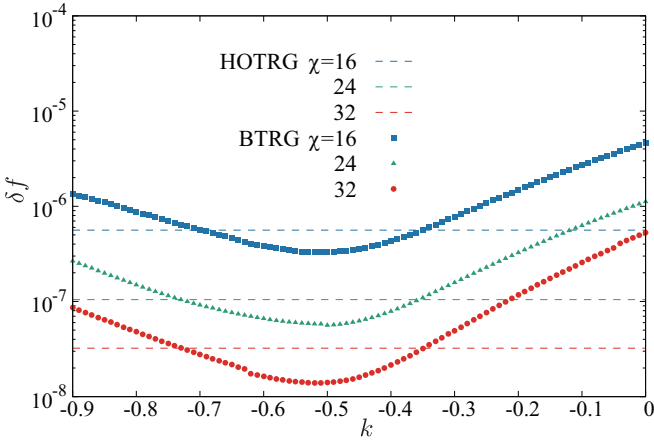


FIG. 2. k dependence of the relative error of the free energy $\delta f = \|f_{\text{calc}} - f_{\text{exact}}\|/\|f_{\text{exact}}\|$ by BTRG at the critical point $\beta = \beta_c$ with $\chi = 16$ (blue squares), 24 (green triangles), and 32 (red circles). The results of HOTRG are also shown by the horizontal lines for comparison.

error of the free energy calculated by BTRG at the critical point $\beta_c = \frac{1}{2} \ln(1 + \sqrt{2})$. As shown in Fig. 2, by setting k negative, we can reduce the relative error from TRG. We do not show the results for $k > 0$ in Fig. 2 as the relative error becomes larger monotonically as k increases. One can see that BTRG gives the best result at $k \approx -0.5$. Moreover, around the optimal point, the result of BTRG becomes more accurate than HOTRG with the same bond dimension χ . In the following calculation, we set k as the optimal value $k = -\frac{1}{2}$.

Next, we consider the χ dependence of the relative error of the free energy at the critical point (Fig. 3). The relative error of the free energy calculated by BTRG is smaller than those by TRG and HOTRG for all bond dimensions. We also see power-law decays $\delta f \propto \chi^{-\alpha}$; the exponent α in BTRG looks larger than those in TRG and HOTRG. We obtain $\alpha \simeq 4.4$ for BTRG, and it is close to the exponent of the finite χ scaling of a matrix product state for the one-dimensional transverse field Ising model [9,28–30]. We also show the β dependence

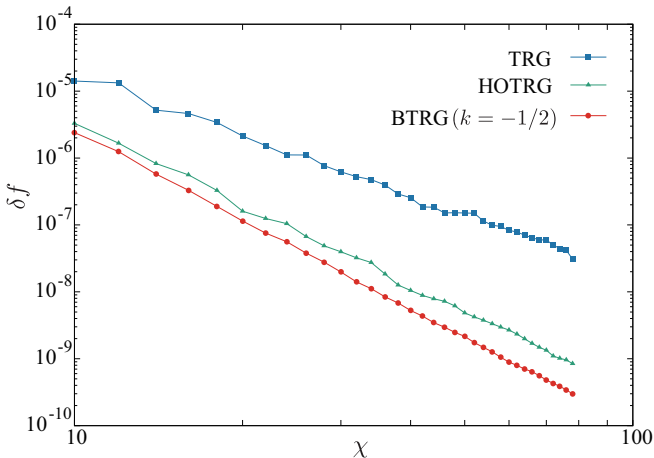


FIG. 3. χ dependence of the relative error of the free energy $\delta f = \|f_{\text{calc}} - f_{\text{exact}}\|/\|f_{\text{exact}}\|$ by TRG (blue squares), HOTRG (green triangles), and BTRG (red circles) at the critical point $\beta = \beta_c$.

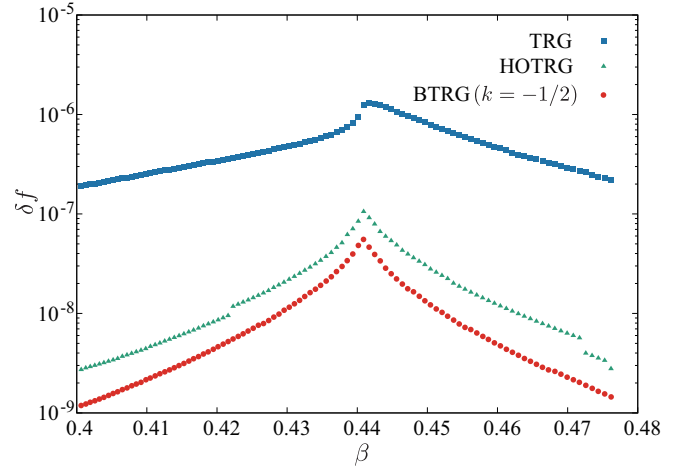


FIG. 4. β dependence of the relative error of the free energy $\delta f = \|f_{\text{calc}} - f_{\text{exact}}\|/\|f_{\text{exact}}\|$ by TRG (blue squares), HOTRG (green triangles), and BTRG ($k = -1/2$) (red circles) for $\chi = 24$.

of the relative error of the free energy in Fig. 4. The bond dimension is $\chi = 24$. Again, the relative error of BTRG is smaller than those by TRG and HOTRG at all temperatures. To further clarify the accuracy of BTRG, we show the χ dependence of the relative error of the energy at the critical point in Fig. 5. Here, the energy is calculated by using the automatic differentiation technique [32]. Similar to the case of free energy, the error of the BTRG is smaller than those of TRG and HOTRG, although we see the energy calculation suffers from relatively more fluctuations.

We, thus, conclude that BTRG outperforms TRG and HOTRG for the square-lattice tensor networks from the above benchmark results. It should be emphasized that the computation cost of BTRG is $O(\chi^5)$, which is the same as TRG and much smaller than that of HOTRG $O(\chi^7)$. Even though the improvement of BTRG over HOTRG is not that impressive

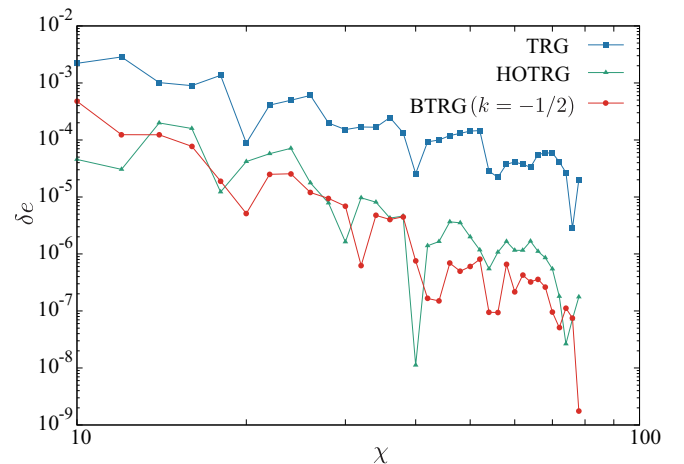


FIG. 5. χ dependence of the relative error of the energy $\delta e = \|e_{\text{calc}} - e_{\text{exact}}\|/\|e_{\text{exact}}\|$ by TRG (blue squares), HOTRG (green triangles), and BTRG (red circles) at the critical point $\beta = \beta_c$. Numerically exact energy for $L = 2^{16}$ is $e = -1.414\,223\,060\,05$ [31].

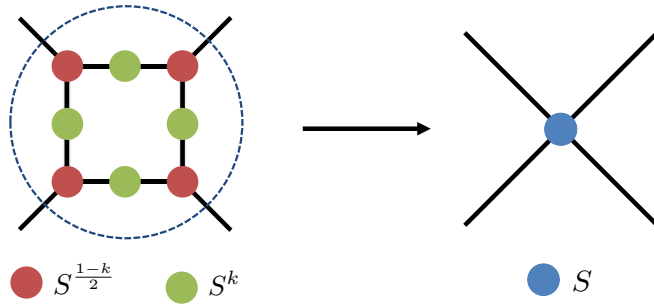


FIG. 6. Singular values of the fixed-point tensors in BTRG. After the tensor decomposition [Eqs. (1)–(8)], we obtain rank-3 tensors with singular values $\sigma^{(1-k)/2}$ and rank-2 tensors with singular values σ^k . By contracting these tensors, a renormalized rank-4 tensor is created, which has the same singular values (σ) as the rank-4 tensor before the renormalization.

with the same bond dimension χ , the difference in the accuracy per computation cost becomes significant for large χ .

As discussed already, one may attribute the improvement of accuracy in BTRG to the effectively larger environment through the bond weights. However, it is not trivial why $k \approx -\frac{1}{2}$ gives the optimal result. Here, we discuss the reason by considering the stationary condition of the renormalization transformation.

We assume that the tensors T , S_1 , and S_2 have already converged to some fixed-point tensors after several renormalization steps. As a result, the singular value matrix σ in Eqs. (1) and (2) as well as the new bond tensors $E = F = \sigma^k$ in Eqs. (4) and (7) become invariant. Then, the renormalized site tensor T' is created from four rank-3 tensors, which are proportional to $\sigma^{(1-k)/2}$, and four rank-2 tensors. If we further assume that the unitary matrices do not contribute to the singular value spectrum, we have the following stationary condition:

$$[\sigma^{(1-k)/2}]^4 [\sigma^k]^4 = \sigma. \quad (12)$$

By solving this equation, we obtain $k = -\frac{1}{2}$ that gives a stable fixed point.

Note that when we assume the corner double line (CDL) structure for the fixed-point tensors where each index consists of two lines representing the corner correlations, one of the two lines is absorbed as a normalization constant after one renormalization step. This fact indicates that only $[\sigma^{(1-k)/2}]^{1/2}$ from each tensor contributes to the singular value spectrum of the renormalized tensor (see Fig. 6). In this case, $k = 0$ satisfies the stationary condition, which is consistent with the previous discussions that the CDL tensor is a fixed point in the conventional TRG [2,18].

We can regard $k = -\frac{1}{2}$ as a necessary condition for the existence of a nontrivial stationary solution of BTRG. Interestingly, the condition $k = -\frac{1}{2}$ gives a scaling of the partition function $Z \propto \sigma^0$, which indicates the scale invariance of the free-energy density. It is another evidence that supports $k = -\frac{1}{2}$ is optimal.

To confirm the stability of the singular value spectrum, here, we show that singular values obtained in BTRG with $k = -\frac{1}{2}$ at the critical point of the two-dimensional Ising

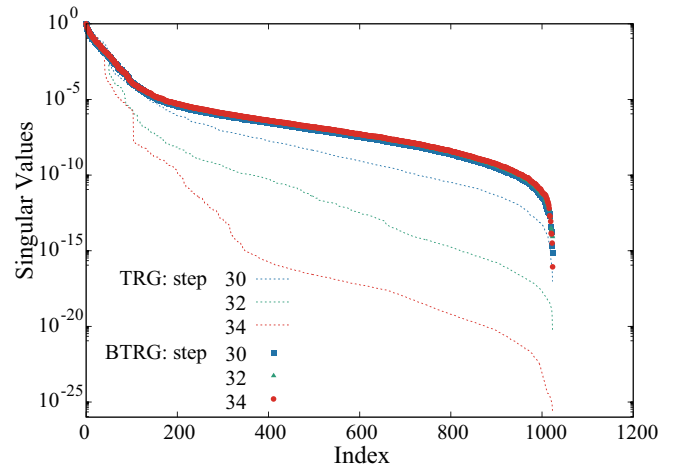


FIG. 7. Singular value spectrum obtained by TRG (dashed lines) and BTRG (symbols) after 30, 32, and 34 renormalization steps corresponding to $L = 2^{15}$, $L = 2^{16}$, and $L = 2^{17}$, respectively. The bond dimension is $\chi = 32$ in all the cases. The singular value spectrum obtained by TRG changes as the renormalization proceeds, whereas the spectrum obtained by BTRG does not exhibit any visible change in this scale.

model. First, we prepare the site tensor after 30, 32, and 34 iterations by TRG and BTRG with $\chi = 32$. Then, the singular value spectrum is calculated by Eq. (1). In Fig. 7, we observe that the spectrum calculated by TRG changes as the renormalization proceeds, whereas that obtained by BTRG shows no significant change. This result strongly supports the above argument that BTRG keeps the scale-invariant structure of tensors at the critical point.

The stability of the singular value spectrum also means the scaling dimensions calculated from the local tensors such as Ref. [18] are stable under the renormalization. Several works have indicated that removing the short-range entanglement is crucial to obtain the scaling dimensions stably [16–26]. However, by using BTRG, we can calculate scaling dimensions stably, without explicitly removing the short-range entanglement. It is another significant property of BTRG.

In this Letter, we proposed a new tensor renormalization-group method BTRG. By considering a network where tensors locate on the sites and bonds, we generalized the original TRG. This approach requires $O(\chi^5)$ computation cost and $O(\chi^3)$ memory footprint, both of which are the same as TRG. Nevertheless, BTRG gives more accurate results with the optimal hyperparameter $k = -\frac{1}{2}$ than not only TRG, but also HOTRG. We showed that the stationary condition could explain the optimal hyperparameter $k = -\frac{1}{2}$ for nontrivial fixed-point tensors. Indeed, we confirmed that the singular value spectrum at the critical point obtained by BTRG with $k = -\frac{1}{2}$ becomes invariant under the renormalization.

In BTRG, by generalizing the tensor network to include bond tensors, site tensors naturally take the environment's effect into account at the decomposition procedure. It contributes to increasing the accuracy of the approximation. This idea can be easily applied to the other tensor renormalization groups, such as TRG on the honeycomb lattice and HOTRG [33]. When we need to keep symmetries of

tensors, a tensor network with explicit bond tensors often appears [34]. One might apply the BTRG idea also to such tensor networks, even if some of their bond weights are not positive.

The nature of the fixed-point tensor in BTRG (with $k = -\frac{1}{2}$) is one of the essential issues to be investigated. As we have shown, the singular value spectrum becomes scale invariant, indicating that it contains detailed critical properties. By understanding the structure of the fixed-point tensors, we might extract the scaling dimensions and fusion rules in the conformal field theory.

We thank K. Harada, N. Kawahima, and H.-H. Zhao for fruitful discussion. D.A. was supported by the Japan Society for the Promotion of Science through the Program for Lead-

ing Graduate Schools (MERIT). T.O. and S.T. acknowledge support from the Endowed Project for Quantum Software Research and Education, The University of Tokyo ([35]). This work was partially supported by MEXT as an ‘‘Exploratory Challenge on a Post-K computer’’ (Frontiers of Basic Science: Challenging the Limits) and ‘‘Program for Promoting Researches on the Supercomputer Fugaku’’ (Basic Science for Emergence and Functionality in Quantum Matter –Innovative Strongly Correlated Electron Science by Integration of ‘‘Fugaku’’ and Frontier Experiments), by JSPS KAKENHI Grants No. 15K17701, No. 17K05564, No. 19K03740, and No. 20H00122, and by JST, PRESTO Grant No. JPMJPR1912, Japan. Parts of the computations were carried out using the facilities of Supercomputer Center, the Institute for Solid State Physics, the University of Tokyo.

-
- [1] L. Onsager, Crystal statistics. I. A two-dimensional model with an order-disorder transition, *Phys. Rev.* **65**, 117 (1944).
- [2] M. Levin and C. P. Nave, Tensor Renormalization Group Approach to Two-Dimensional Classical Lattice Models, *Phys. Rev. Lett.* **99**, 120601 (2007).
- [3] W. Li, S.-S. Gong, Y. Zhao, S.-J. Ran, S. Gao, and G. Su, Phase transitions and thermodynamics of the two-dimensional Ising model on a distorted kagome lattice, *Phys. Rev. B* **82**, 134434 (2010).
- [4] Q. N. Chen, M. P. Qin, J. Chen, Z. C. Wei, H. H. Zhao, B. Normand, and T. Xiang, Partial Order and Finite-Temperature Phase Transitions in Potts Models on Irregular Lattices, *Phys. Rev. Lett.* **107**, 165701 (2011).
- [5] B. Dittrich and F. C. Eckert, Towards computational insights into the large-scale structure of spin foams, *J. Phys.: Conf. Ser.* **360**, 012004 (2012).
- [6] G. Evenbly and G. Vidal, Local Scale Transformations on the Lattice with Tensor Network Renormalization, *Phys. Rev. Lett.* **116**, 040401 (2016).
- [7] S. Wang, Z.-Y. Xie, J. Chen, N. Bruce, and T. Xiang, Phase transitions of ferromagnetic Potts models on the simple cubic lattice, *Chin. Phys. Lett.* **31**, 070503 (2014).
- [8] J. F. Yu, Z. Y. Xie, Y. Meurice, Y. Liu, A. Denblyker, H. Zou, M. P. Qin, J. Chen, and T. Xiang, Tensor renormalization group study of classical XY model on the square lattice, *Phys. Rev. E* **89**, 013308 (2014).
- [9] H. Ueda, K. Okunishi, and T. Nishino, Doubling of entanglement spectrum in tensor renormalization group, *Phys. Rev. B* **89**, 075116 (2014).
- [10] J. Genzor, A. Gendiar, and T. Nishino, Phase transition of the Ising model on a fractal lattice, *Phys. Rev. E* **93**, 012141 (2016).
- [11] L.-P. Yang, Y. Liu, H. Zou, Z. Y. Xie, and Y. Meurice, Fine structure of the entanglement entropy in the O(2) model, *Phys. Rev. E* **93**, 012138 (2016).
- [12] H. Kawachi and S. Takeda, Tensor renormalization group analysis of CP(N – 1) model, *Phys. Rev. D* **93**, 114503 (2016).
- [13] Z. Y. Xie, H. C. Jiang, Q. N. Chen, Z. Y. Weng, and T. Xiang, Second Renormalization of Tensor-Network States, *Phys. Rev. Lett.* **103**, 160601 (2009).
- [14] H. H. Zhao, Z. Y. Xie, Q. N. Chen, Z. C. Wei, J. W. Cai, and T. Xiang, Renormalization of tensor-network states, *Phys. Rev. B* **81**, 174411 (2010).
- [15] Z. Y. Xie, J. Chen, M. P. Qin, J. W. Zhu, L. P. Yang, and T. Xiang, Coarse-graining renormalization by higher-order singular value decomposition, *Phys. Rev. B* **86**, 045139 (2012).
- [16] G. Evenbly and G. Vidal, Tensor Network Renormalization, *Phys. Rev. Lett.* **115**, 180405 (2015).
- [17] S. Yang, Z.-C. Gu, and X.-G. Wen, Loop Optimization for Tensor Network Renormalization, *Phys. Rev. Lett.* **118**, 110504 (2017).
- [18] Z.-C. Gu and X.-G. Wen, Tensor-entanglement-filtering renormalization approach and symmetry-protected topological order, *Phys. Rev. B* **80**, 155131 (2009).
- [19] G. Evenbly, Algorithms for tensor network renormalization, *Phys. Rev. B* **95**, 045117 (2017).
- [20] K. Harada, Entanglement branching operator, *Phys. Rev. B* **97**, 045124 (2018).
- [21] M. Bal, M. Mariën, J. Haegeman, and F. Verstraete, Renormalization Group Flows of Hamiltonians using Tensor Networks, *Phys. Rev. Lett.* **118**, 250602 (2017).
- [22] M. Hauru, C. Delcamp, and S. Mizera, Renormalization of tensor networks using graph-independent local truncations, *Phys. Rev. B* **97**, 045111 (2018).
- [23] C. Wang, S.-M. Qin, and H.-J. Zhou, Topologically invariant tensor renormalization group method for the Edwards-Anderson spin glasses model, *Phys. Rev. B* **90**, 174201 (2014).
- [24] H.-H. Zhao, Z.-Y. Xie, T. Xiang, and M. Imada, Tensor network algorithm by coarse-graining tensor renormalization on finite periodic lattices, *Phys. Rev. B* **93**, 125115 (2016).
- [25] G. Evenbly, Gauge fixing, canonical forms, and optimal truncations in tensor networks with closed loops, *Phys. Rev. B* **98**, 085155 (2018).
- [26] A. J. Ferris, Area law and real-space renormalization, *Phys. Rev. B* **87**, 125139 (2013).
- [27] D. Adachi, T. Okubo, and S. Todo, Anisotropic tensor renormalization group, *Phys. Rev. B* **102**, 054432 (2020).
- [28] L. Tagliacozzo, T. R. de Oliveira, S. Iblisdir, and J. I. Latorre, Scaling of entanglement support for matrix product states, *Phys. Rev. B* **78**, 024410 (2008).
- [29] F. Pollmann, S. Mukerjee, A. M. Turner, and J. E. Moore, Theory of Finite-Entanglement Scaling at One-Dimensional Quantum Critical Points, *Phys. Rev. Lett.* **102**, 255701 (2009).

- [30] B. Pirvu, G. Vidal, F. Verstraete, and L. Tagliacozzo, Matrix product states for critical spin chains: Finite-size versus finite-entanglement scaling, *Phys. Rev. B* **86**, 075117 (2012).
- [31] <https://github.com/todo-group/exact>.
- [32] H.-J. Liao, J.-G. Liu, L. Wang, and T. Xiang, Differentiable Programming Tensor Networks, *Phys. Rev. X* **9**, 031041 (2019).
- [33] See Supplemental Material at <http://link.aps.org/supplemental/10.1103/PhysRevB.105.L060402> for the application of BTRG to TRG on the honeycomb lattice and HOTRG.
- [34] K. Harada, Universal spectrum structure at nonequilibrium critical points in the (1+1)-dimensional directed percolation, [arXiv:2008.10807](https://arxiv.org/abs/2008.10807).
- [35] <https://qsw.phys.s.u-tokyo.ac.jp/>.